*Transactions*, SMiRT-22
San Francisco, California, USA - August 18-23, 2013
Division II

# LOWER THRESHOLD LHGR FOR INITIATION OF OUTSIDE-IN RADIAL CRACKS IN LINER FUEL CLADDING

**Lars O. Jernkvist**[1,2]

[1] Consulting scientist, Quantum Technologies AB, Uppsala, Sweden (loje@quantumtech.se)
[2] Visiting research associate, Division of Materials Science, Malmö University, Malmö, Sweden

## ABSTRACT

Based on the hypothesis that precipitation and growth of radially aligned hydrides at the metal-oxide interface is a necessary step for initiation of outside-in radial cracks in liner cladding tubes of high-burnup boiling water reactor fuel rods, simple analytical solutions are used to formulate a necessary condition for this kind of cladding failures in terms of a threshold for the fuel rod linear heat generation rate. The formulation rests on conservative assumptions, and comparisons with results from two independent series of power ramp tests confirm that the derived threshold may serve as a lower bound failure criterion. Calculated results also suggest that current 9×9 and 10×10 fuel designs are less susceptible to outside-in cladding failure than older 8×8 designs. The calculated lower bound failure threshold for modern 10×10 designs is 40-42 $kWm^{-1}$.

## INTRODUCTION

The frequency of fuel rod failures in light water reactors have constantly decreased over the years, thanks to improvements in fuel designs, in-core fuel management procedures and reactor operating rules (Zinkle and Was, 2013). One important design improvement is the introduction of so called liner cladding, which has effectively reduced fuel rod failures caused by pellet-cladding interaction (PCI). This failure mechanism comprises both mechanical interaction of the expanding fuel pellets with the cladding tube that encases the pellets, and chemical interaction between the cladding and aggressive fission products (notably iodine) released from the fuel (Cox, 1990). The combination of these effects may result in stress corrosion cracking (SCC), leading to inside-out radial crack growth through the cladding wall. The failures typically occur when the fuel rod linear heat generation rate (LHGR) is rapidly increased, which induces high tensile stress in the cladding by strong pellet-cladding mechanical interaction (PCMI).

Cladding failures by PCI have historically been more frequent in boiling water reactors (BWRs) than in pressurized water reactors (PWRs), due to the difference in reactivity control between the two reactor types. Consequently, liner cladding is mostly used in BWRs as a remedy against PCI failures. Liner cladding tubes for BWR fuel have a soft inner layer (liner) of almost pure zirconium, which is metallurgically bond to the Zircaloy-2 (Zr-1.5Sn-0.14Fe-0.12O-0.10Cr-0.05Ni by wt%) base metal. The soft liner layer, which is typically about 100 μm thick, improves the resistance to PCI-induced failures partly by reducing stress concentrations imposed by PCMI, but the liner material is also less susceptible to iodine-induced SCC than the Zircaloy-2 base metal.

Liner cladding has proven to be an efficient remedy against failures caused by inside-out radial crack growth by SCC. However, results from recent power ramp tests show that high-burnup BWR fuel rods with liner cladding may still fail during overpower transients. The observed failures are caused by *outside-in* radial crack growth (Hayashi et al., 2006, Alvarez-Holston et al., 2010). Examinations of the failed rods suggest that the cracks initiate from radially oriented precipitates of zirconium hydride or from

densely hydrided regions at the cladding outer surface (Shimada et al., 2004), and that the cracks grow in the radial-axial direction by DHC - delayed hydride cracking (Puls, 2012). Failures of this kind have been observed in a handful of power ramp tests, all of which have been carried out with high (> 42 $kWm^{-1}$) ramp terminal power and with liner cladding BWR fuel rods of high (> 56 $MWd(kgU)^{-1}$) burnup.

To the author's best knowledge, there are currently no engineering type failure criteria for outside-in failures of liner cladding by delayed hydride cracking. Such criteria are needed in fuel rod analysis software for assessing the risk for cladding failure during various operating conditions. They must capture the essentials of the failure process, without being computationally oppressive. Available results from ramp tests suggest that engineering type failure criteria for outside-in radial DHC in liner cladding tubes should focus first and foremost on the crack initiation stage: From post-test examinations reported in the aforementioned references, it is clear that surface flaws through the cladding waterside oxide layer and the subjacent rim of densely hydrided metal exist in large numbers. In contrast, it seems that there are very few observations of incipient radial cracks that extend *beyond* the hydride rim at the metal-oxide interface. These results suggest that initiation of radial cracks into the ductile metal beneath the hydride rim is a crucial and necessary step in the failure process. This hypothesis forms the basis for the present work, in which a lower bound engineering-type failure criterion for outside-in failure of liner cladding to high-burnup BWR fuel rods is formulated.

## MODEL FOR INITIATION OF OUTSIDE-IN RADIAL CRACKS IN THE CLADDING

### *Prerequisites and Fundamental Assumptions*

We consider liner cladding tubes of high-burnup BWR fuel rods, which have picked up a substantial amount of hydrogen by metal-water reactions during in-reactor operation. Since the hydrogen solid solubility is low in zirconium alloys, the considered material will contain precipitates of zirconium hydrides, which are predominantly in the δ-phase (Kammenzind et al., 1996). A typical distribution of δ-hydride precipitates is shown at the top of figure 1. A rim of hydrides is usually found beneath the waterside oxide layer at the cladding outer surface, and another hydride rim is found in the liner layer, at the interface with the cladding base metal. The outer hydride rim forms during normal reactor operation, as a consequence of the radial temperature gradient across the cladding wall. The hydride rim in the liner, however, forms during zero-power operation and slow cooling to cold shutdown of the reactor. The phenomenon, which has been studied experimentally by Takagi et al. (1996), is caused by a lower solid solubility for hydrogen in the liner than in the base metal.

For high-burnup fuel rods with liner cladding that exhibit typical hydride distributions as shown in figure 1, we may derive a threshold LHGR for initiation of outside-in radial cracks, based on the following hypothetical scenario: i) During a reactor power excursion, hydrides at the liner interface dissolve due to the temperature increase. The concentration of hydrogen in solid solution at the interface will be equal to the hydrogen solid solubility for the liner material, as long as some hydrides remain un-dissolved at the interface. ii) Hydrogen in solid solution flows from the liner interface towards the cladding outer surface as a result of the temperature gradient, and towards flaws and other stress concentrators at the cladding outer surface as a result of stress gradients. Hydrogen will cease to flow when equilibrium is reached. This occurs when the gradient in hydrogen concentration balances the temperature and stress gradients within the material. iii) Radially aligned hydrides form ahead of the aforementioned stress concentrators, when the hydrogen solid solubility is locally transgressed. iv) The hydrides grow radially inwards from the cladding outer surface and eventually break as a result of tensile hoop stress, thus initiating a sharp outside-in radial crack in the cladding.

This scenario for initiation of outside-in radial cracks is supported by results of recent out-of-reactor tests on BWR liner cladding with high concentrations of hydrides in the liner material (Ogata et al., 2009). These tests also show that a sufficient temperature gradient is needed across the cladding wall for hydrides to form at the cladding outer surface. This observation, together with the assumptions i)-iv), is in the following used to derive a *necessary* condition for initiation of outside-in radial cracks in terms of a threshold for the fuel rod LHGR. Based on data for fundamental material properties and simple analytical solutions for the stationary distributions of temperature and hydrogen in the cladding, together with similar solutions for the local stress distribution at flaws, we calculate the lowest conceivable LHGR for which crack initiation may occur.

***Mathematical Formulation***

Let us start by considering the hydrogen flux, $\bar{J}$, by interstitial diffusion in the Zircaloy-2 base metal of the cladding tube. In absence of stress gradients, it can be written (Shewmon, 1989)

$$\bar{J} = -D_m\left( \nabla C_m + \frac{C_m Q_m^*}{RT^2}\nabla T \right), \quad (1)$$

where $C_m$ is the concentration of hydrogen in solid solution within the metal, $D_m$ and $Q_m^*$ are the hydrogen diffusivity and heat of transport in the metal, $T$ is the absolute temperature and $R$ is the universal gas constant. A stationary (equilibrium) solution to the distribution of hydrogen in solid solution within the cladding base metal can be found by setting $\bar{J} = 0$ in eq. (1). The result is

$$C_m(\bar{r}) = A\exp\left( \frac{Q_m^*}{RT(\bar{r})} \right), \quad (2)$$

where $A$ is a constant that can be determined from boundary conditions. Equation (2) implies that the stationary distribution of hydrogen in solid solution is controlled by the stationary temperature distribution in the cladding metal. Assuming axial symmetry, the latter can with fair accuracy be written

$$T(r) = T_{mo} + \frac{q'}{2\pi\lambda_m}\ln(R_{mo}/r), \quad (3)$$

where $r$ is the radial coordinate, $R_{mo}$ is the radial position of the metal-oxide interface at the cladding outer surface, $T_{mo}$ is the temperature at this position, $q'$ is the fuel rod LHGR and $\lambda_m$ is the thermal conductivity of the cladding metal. The latter is slightly temperature dependent, but here assumed to be constant. The metal-oxide interface temperature may be calculated from the oxide surface temperature, $T_o$, through

$$T_{mo} = T_o + \frac{q'}{2\pi\lambda_o}\ln(R_o/R_{mo}), \quad (4)$$

where $R_o$ is the radial position of the oxide surface and $\lambda_o$ is the thermal conductivity of the oxide.

By combining eqs. (2)-(4), it is possible to calculate the stationary distribution of hydrogen in solid solution within the cladding base metal, provided that $q'$, $\lambda_m$, $\lambda_o$, $T_o$ and the cladding tube dimensions are known. In addition, a boundary condition is needed to determine the constant $A$ in eq. (2). This boundary condition is given by assumption i) in the preceding subsection: If hydrides exist in the liner at the interface to the base metal, and if they have been partly dissolved by the temperature increase during a reactor power excursion, then $C_m$ at the interface must equal the hydrogen solid solubility for hydride dissolution in the liner material, $S_l^D$. The boundary condition is thus given by $C_m(R_{lm}) = S_l^D(T_{lm})$, where $R_{lm}$ and $T_{lm}$ is the radial position and temperature, respectively, of the liner-metal interface; see figure 1.

By substituting this boundary condition into eq. (2), we get

$$C_m(r) \;=\; S_l^D(T_{lm}) \exp\left( \frac{Q_m^*}{RT(r)} - \frac{Q_m^*}{RT_{lm}} \right) . \qquad (5)$$

The solution given by eq. (5) is plotted in figure 1 for a typical case with $q'$ = 40 kWm$^{-1}$, $T_o$=560 K, and fuel rod cladding dimensions typical for a modern 10×10 assembly design ($R_i$=4.315 mm, $R_o$=4.920 mm). The liner and oxide layer thicknesses are here assumed to be 90 µm and 20 µm, respectively. The material properties used in the calculations are listed in table 1. Also included in figure 1 are the calculated hydrogen solid solubilities for hydride dissolution (superscript *D*) and precipitation (superscript *P*). These solubilities depend on temperature and material composition. They are lower in the liner ($S_l^D$ and $S_l^P$) than in the Zircaloy-2 base metal ($S_m^D$ and $S_m^P$); see table 1.

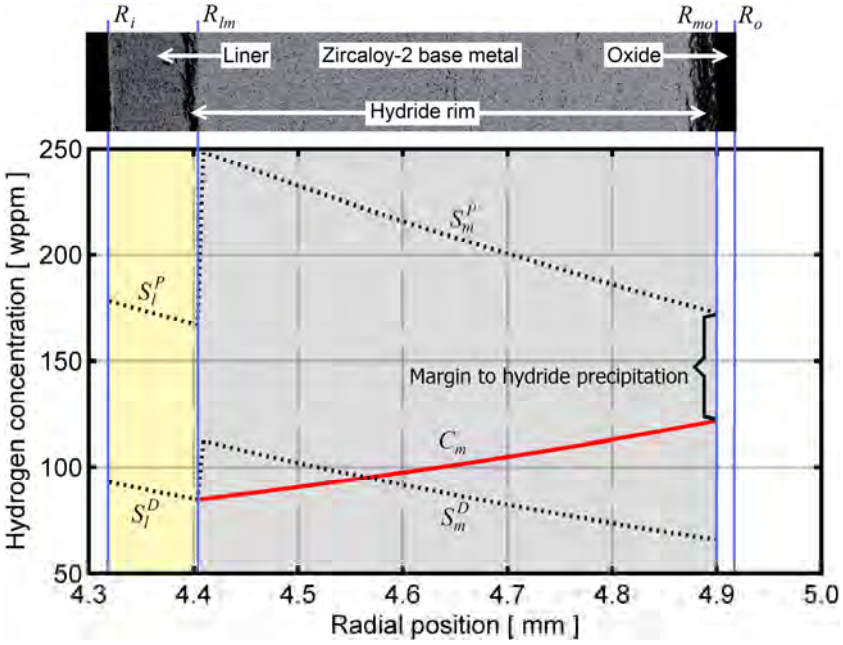


Figure 1: Bulk distribution of hydrogen in solid solution under stationary condition, $C_m$, calculated for a typical 10×10 BWR liner cladding design; see text for details. The indicated margin to hydride precipitation at the metal-oxide interface may decrease substantially at positions with high hydrostatic stress, e.g. at flaws or other stress concentrators. A typical hydride distribution in liner cladding to high-burnup BWR fuel rods is shown in the upper part of the figure.

Hydrides may precipitate at the metal-oxide interface if $C_m$ reaches the hydrogen solid solubility for hydride precipitation, $S_m^P$. For the case considered in figure 1, it is clear that there is a significant margin for this to occur. However, $C_m$ shown in figure 1 pertains to the *bulk* concentration of hydrogen in solid solution. Since hydrogen diffuses towards regions with high hydrostatic stress, the *local* concentration of hydrogen in solid solution may be higher at flaws or other stress concentrators in the cladding metal, and the solid solubility may therefore be locally transgressed at these positions. The local equilibrium value for $C_m$ at a stress concentrator, $C_m^+$, can be written (Li et al.,1966)

$$C_m^+ \;=\; C_m \exp\left( \frac{\Delta\sigma_{kk} V_m^H}{3RT} \right) , \qquad (6)$$

where $\Delta\sigma_{kk}$ is the difference in stress trace between the position of the stress concentrator and the surrounding bulk material, and $V_m^H$ is the partial molar volume of hydrogen in the metal; see table 1. A necessary condition for local precipitation of hydrides ahead of a stress concentrator at the oxide-metal interface is that $C_m^+ \geq S_m^P$ at $r = R_{mo}$. By combining eqs. (5) and (6), the condition can be written

$$S_l^D(T_{lm}) \exp\left( \frac{Q_m^*}{RT_{mo}} - \frac{Q_m^*}{RT_{lm}} + \frac{\Delta\sigma_{kk} V_m^H}{3RT_{mo}} \right) \geq S_m^P(T_{mo}) \quad . \tag{7}$$

The temperatures at either side of the cladding base metal layer, $T_{lm}$ and $T_{mo}$ in eq. (7), can be calculated through eqs. (3) and (4) or by use of a computer program for fuel rod thermal analysis. They depend on cladding tube dimensions, oxide surface temperature, oxide layer thickness and the fuel rod LHGR.

Equation (7) may be applied as a necessary condition for local hydride precipitation, and thus for initiation of outside-in cladding cracks, if $\Delta\sigma_{kk}$ can be calculated for real or assumed stress concentrators at the metal-oxide interface. A conservative estimate (highest possible value for $\Delta\sigma_{kk}$ and lowest possible margin for bulk hydride precipitation, $S_m^P$-$C_m$) is obtained by assuming a sharp radial flaw through the oxide layer, with its tip in the hydride rim just beneath the metal-oxide interface. In this case, $\Delta\sigma_{kk} \approx B\sigma_m^y - \sigma_{kk}^o$, where $\sigma_m^y$ is the yield strength of the cladding metal, $\sigma_{kk}^o$ is the stress trace in the surrounding bulk metal and $B$ is a parameter that depends on the material's strain hardening. For highly irradiated Zircaloy-2, the strain hardening is negligible, and $B$ is approximately $\sqrt{3}(1+\pi)$. This value is obtained for sharp cracks in perfectly rigid plastic materials (Kanninen and Popelar, 1985). Higher values for $B$ are obtained for materials that exhibit strain hardening (Rice and Rosengren, 1968). Finally, we may estimate the stress trace in the bulk metal far away from the flaw, $\sigma_{kk}^o$, by assuming that the LHGR is sufficiently high to induce PCMI and cladding plastic deformation under equal biaxial stress, i.e. $\sigma_{\varphi\varphi} = \sigma_{zz} = \sigma_m^y$. In this case, we get $\sigma_{kk}^o \approx 2\sigma_m^y$. Hence, a fair approximation for $\Delta\sigma_{kk}$ in a highly irradiated cladding tube material that has very little strain hardening and that deforms plastically by strong PCMI is given by

$$\Delta\sigma_{kk} \approx \sqrt{3}(1+\pi)\sigma_m^y - 2\sigma_m^y \approx 5.17\,\sigma_m^y \quad . \tag{8}$$

A correlation for $\sigma_m^y$ with respect to temperature, fitted to transverse strength data for highly irradiated Zircaloy-2 cladding, is given in table 1. Since we consider flaws and other stress-concentrators at the metal-oxide interface, $\sigma_m^y$ in eq. (8) should be evaluated for $T = T_{mo}$.

Table 1: Material properties used in calculations. Subscripts *m*, *l* and *o* refer to Zircaloy-2 base metal, zirconium liner and zirconium oxide ($ZrO_2$). Here, $T$ is the absolute temperature in kelvin.

| **Property, unit:** | **Value:** | **Source:** |
|---|---|---|
| Thermal conductivity, $\lambda_m$, $W(mK)^{-1}$ | 15.7 | (Hagrman et al., 1981) |
| Thermal conductivity, $\lambda_o$, $W(mK)^{-1}$ | 1.8 | (Hagrman et al., 1981) |
| Heat of transport, $Q_m^*$, $Jmol^{-1}$ | $2.5\times10^4$ | (Sawatzky, 1960) |
| Molar volume of hydrogen, $V_m^H$, $m^3mol^{-1}$ | $1.7\times10^{-6}$ | (Eadie et al., 1992) |
| Yield strength, $\sigma_m^y$, Pa | $1.07\times10^9 - 9.18\times10^5 \cdot T$ | (This work) |
| Hydrogen solubility, dissolution, $S_m^D$, wppm | $1.43\times10^5 \exp(-4412.6/T)$ | (Une et al., 2009) |
| Hydrogen solubility, precipitation, $S_m^P$, wppm | $3.27\times10^4 \exp(-3012.0/T)$ | (Une et al., 2009) |
| Hydrogen solubility, dissolution, $S_l^D$, wppm | $1.41\times10^5 \exp(-4582.9/T)$ | (Une and Ishimoto, 2004) |
| Hydrogen solubility, precipitation, $S_l^P$, wppm | $3.39\times10^4 \exp(-3282.4/T)$ | (Une and Ishimoto, 2004) |

## RESULTS AND DISCUSSION

First, we note that the local concentration of hydrogen in solid solution at the tip of the assumed oxide flaw at the metal-oxide interface is significantly higher than in the surrounding bulk material. For the example considered in figure 1, we get $T_{mo}$=574 K and $\sigma_m^y(T_{mo})$=547 MPa, which inserted into eqs. (6) and (8) yields $C_m^+/C_m$ = 1.40. Hence, the calculated hydrogen concentration is 40% higher at the flaw tip than in the bulk material. For the example in figure 1, the flaw tip hydrogen concentration would reach nearly 170 wppm, which is very close to the local hydrogen solid solubility for hydride precipitation, $S_m^P$. We may therefore conclude that flaws and other stress concentrators at the metal-oxide interface are strong preferential sites for hydride precipitation.

The linear heat generation rate required for hydrides to precipitate at these stress concentrators can be easily estimated through eqs. (7) and (8), making use of the material properties in table 1 and the approximation for the cladding stationary temperature distribution in eqs. (3) and (4). Input data to the calculations are the oxide surface temperature, the cladding tube dimensions, and the liner and oxide layer thicknesses. Figure 2 shows the calculated effect of cladding dimensions on the threshold LHGR for hydride precipitation and crack initiation at the metal-oxide interface. The calculations were done with an assumed oxide surface temperature ($T_o$) of 560 K, and the thicknesses of the liner and oxide layers were assumed to be 90 µm and 20 µm, respectively. These values are typical for high-burnup BWR fuel and normal BWR temperature conditions. The markers included in figure 2 are results, calculated for current 9×9 and 10×10 commercial BWR fuel designs and two older 8×8 designs (NEI, 2004).

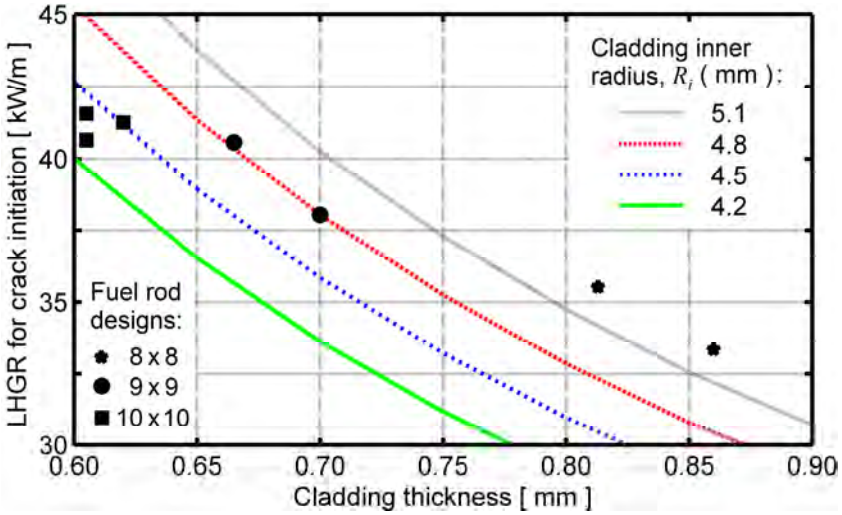


Figure 2: Calculated lower bound threshold LHGR for initiation of outside-in radial cracks in Zircaloy-2 cladding with a 90 µm thick inner surface liner and a 20 µm outer surface oxide layer. An assumed oxide surface temperature of 560 K was used in the calculations.

The results in figure 2 suggest that modern fuel designs with thin-walled cladding tubes are less susceptible to hydride precipitation and radial crack initiation at the metal-oxide interface than older thick-walled 8×8 designs. This result, which is corroborated by findings from out-of-reactor experiments on cladding tubes with different dimensions (Ogata et al., 2009), is a consequence of the differences in bulk hydrogen distribution between thin-walled and thick-walled cladding.

It should be emphasized that the calculated results should be interpreted as a lower bound threshold LHGR for initiation of liner cladding outside-in radial cracks in high-burnup fuel rods; it is *not a sufficient* condition for cladding failure. For the cladding to actually fail at the calculated LHGR, there have to be: i) a sufficient tensile hoop stress in the cladding for eq. (8) to apply and for breaking radially aligned hydrides that form at the metal-oxide interface, ii) a sufficient amount of hydrogen in the cladding for eq. (5) to be valid, and iii) a sufficient hold time at high LHGR for the cladding hydrogen distribution to change, and then for the crack to initiate and propagate radially through the wall of the cladding tube.

Results from power ramp tests on high-burnup BWR fuel rods generally show that the cladding deforms plastically at LHGRs above 30 $kWm^{-1}$ (Alvarez-Holston et al., 2010). Hence, condition i) will always be satisfied for the LHGRs of interest here. For condition ii) to be satisfied, we note from the calculated variation of $C_m$ in figure 1 that a minimum average hydrogen concentration across the cladding wall of about 100 wppm is needed for eq. (5) to be valid and for the local hydrogen concentration at stress concentrators ($C_m^+$) to reach $S_m^P$ at the metal-oxide interface. Finally, we may estimate the time needed for crack propagation by DHC through the cladding wall from reported crack growth rates for irradiated Zircaloy-2 cladding in the temperature range of interest. Efsing and Pettersson (2000) measured crack growth rates up to about 1 $\mu ms^{-1}$ at 573 K, which implies that at least about 10 minutes are needed for a radially growing crack to penetrate the cladding. In addition, a certain time will be needed from start of the power surge to change the hydrogen distribution within the cladding by diffusion towards the cold outer surface and to form hydrides at the metal-oxide interface. We may thus suspect that the hold time at high power must be longer than 10 minutes for the cladding to fail by outside-in radial DHC.

These estimated requirements on minimum hydrogen concentration and hold time at high fuel rod power agree with results from power ramp tests on high-burnup BWR fuel rods with liner cladding. Table 2 summarizes results reported from two different studies. The first series of tests (A-C) were carried out in the R2 reactor in Sweden (Alvarez-Holston et al., 2010). The tested fuel rods were of SVEA-96+ 10×10 design, with $R_i$=4.180 mm and $R_o$=4.810 mm. The lower bound failure threshold for this fuel rod design is 37.8 $kWm^{-1}$, according to calculations with our model. The second series of tests (11-24) were done in the JMTR, Japan (Hayashi et al., 2003 and 2006). The tested fuel rods were of Japanese Step-II 8×8 design, with $R_i$=5.290 mm and $R_o$=6.150 mm. The calculated lower bound failure threshold is 33.3 $kWm^{-1}$ for this fuel rod design (rightmost marker in figure 2). Both single-step and multi-step (staircase) power ramps were used in both series of tests. All failures included in table 2 were caused by outside-in crack growth along the radial-axial plane of the cladding tube. It is clear from table 2 that no failures occurred for hold times shorter than 22 minutes. With the exception of test 15, no failures occurred for cladding hydrogen concentrations lower than 100 wppm. Moreover, all observed failures occurred at LHGRs that are higher than our calculated failure thresholds for the two fuel designs, which confirms that our model assumptions provide a lower bound threshold for the observed kind of failures.

The calculated threshold for crack initiation at the cladding metal-oxide interface depends also on the cladding oxide layer thickness and the oxide surface temperature, but the dependence is weak. This is illustrated by figure 3, which shows the calculated threshold for a 10×10 fuel rod with $R_i$=4.315 mm, $R_o$=4.920 mm and a 90 μm thick liner; this is the same design as used for the example in figure 1. Obviously, the considered ±10 K variation in oxide surface temperature results in a practically negligible ($< \pm 0.3$ $kWm^{-1}$) variation of the calculated failure threshold. The calculated effect of oxide layer thickness is somewhat stronger. The reason is that a thick oxide layer implies a reduction of the cladding metal thickness, at the same time as the metal temperature increases and the yield strength therefore decreases. Both these effects contribute to the calculated increase in failure threshold with increasing oxide thickness.

Table 2: Summary of power ramp tests, carried out on high-burnup BWR fuel rods with liner cladding in the R2 reactor (tests A-C) and the JMTR (tests 11-24). Tests A-C were done on 10×10 type fuel rods (Alvarez-Holston et al., 2010), while tests 11-24 were done on 8×8 rods (Hayashi et al., 2003 and 2006). SS: Single-step, MS: Multi-step, $\Delta q'$ : Power step in ramp, RTP: Ramp terminal power.

| Test ID | Rod burnup [ MWd(kgU)$^{-1}$ ] | Hydrogen [ wppm ] | Ramp type | $\Delta q'$ [ kWm$^{-1}$] | RTP [ kWm$^{-1}$ ] | Hold time [ min ] | Test result |
|---|---|---|---|---|---|---|---|
| A | 62 | 208 | MS | 5.0 | 42 | 40 | Failed |
| B | 66 | 270 | SS | 29 | 41 | 0.5 | Survived |
| C | 56 | 70 | MS | 5.0 | 52 | 720 | Survived |
| 11 | 56.3 | 70-100 | MS | 5.0 | 59.2 | 240 | Survived |
| 12 | 56.3 | 70-100 | SS | 13.0 | 35.0 | 240 | Survived |
| 13 | 56.3 | 70-100 | SS | 21.2 | 43.2 | 10 | Survived |
| 14 | 56.2 | 70-100 | SS | 21.3 | 43.3 | 240 | Survived |
| 15 | 56.3 | 70-100 | SS | 26.8 | 55.1 | 146 | Failed |
| 16 | 56.2 | 70-100 | SS | 24.0 | 50.1 | 240 | Survived |
| 17 | 60.8 | 110-160 | MS | 5.0 | 44.6 | 22 | Failed |
| 18 | 60.8 | 110-160 | SS | 13.2 | 33.3 | 240 | Survived |
| 19 | 60.8 | 110-160 | SS | 18.5 | 39.9 | 240 | Survived |
| 20 | 59.5 | 100-130 | SS | 19.5 | 39.9 | 10 | Survived |
| 21 | 59.5 | 100-130 | SS | 17.0 | 33.6 | 19260 | Survived |
| 22 | 61.1 | 110-180 | SS | 21.8 | 42.1 | 100 | Survived |
| 23 | 61.1 | 110-180 | SS | 20.0 | 40.2 | 240 | Survived |
| 24 | 61.1 | 110-180 | SS | 22.6 | 42.8 | 68 | Failed |

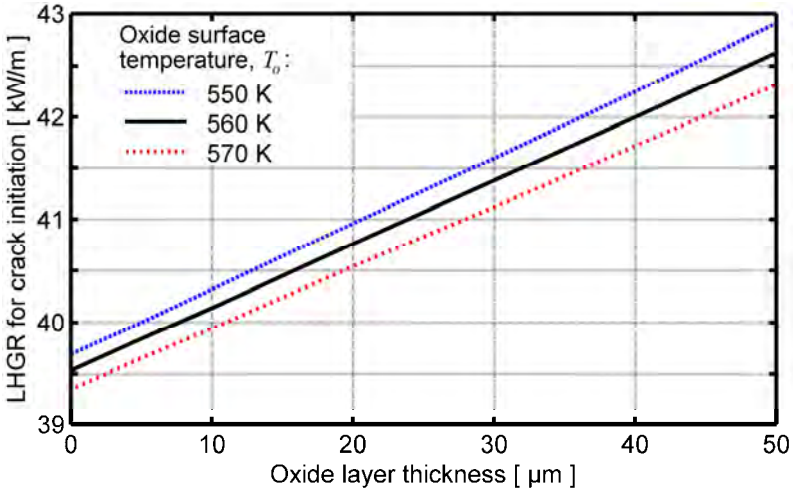


Figure 3: Calculated effect of oxide layer thickness and oxide surface temperature on the lower bound threshold LHGR for crack initiation in a typical 10×10 BWR liner cladding design; see text for details.

## CONCLUSIONS

A necessary condition for initiation of outside-in radial cracks in liner cladding tubes to high-burnup BWR fuel rods was formulated. The formulation rests on the assumptions that formation of radially aligned hydrides at the cladding metal-oxide interface is a necessary step for crack initiation, and that redistribution of hydrogen from the liner layer to the metal-oxide interface plays a key role in this process. Based on these assumptions, data for fundamental material properties and simple analytical solutions for the stationary distributions of temperature and hydrogen in the cladding, together with similar solutions for the local stress distribution around flaws at the metal-oxide interface, the lowest conceivable LHGR required for crack initiation can be calculated for a given fuel rod design. Comparisons with results from power ramp tests on high-burnup BWR fuel rods with liner cladding confirm the conservative nature of the derived failure threshold. It should be remarked that no empirical fitting parameters were used in the derivation of the failure threshold.

Calculations presented in this work suggest that modern 10×10 BWR fuel designs are less susceptible to outside-in cladding failure than older 8×8 designs, as a result of the differences in cladding wall thickness. The calculated lower bound failure threshold is 40-42 $kWm^{-1}$ for modern 10×10 designs, but merely 33-36 $kWm^{-1}$ for old 8×8 designs. These results imply that care must be taken when establishing empirical failure criteria from ramp test data. For instance, failure thresholds fitted to ramp test data for old 8×8 fuel designs may be unnecessarily restrictive for modern 10×10 designs.

Finally, it should be remarked that the calculated failure threshold provides a *necessary*, but not a *sufficient* condition for cladding failure by outside-in DHC. For failure to actually occur at the calculated threshold LHGR, approximate analyses suggest that a radial average hydrogen concentration in the cladding of at least 100 wppm is needed, and that the fuel rod power must be maintained for at least 10 minutes to allow time for radial crack growth through the cladding wall. Analyses with an advanced computational model (Jernkvist and Massih, 2007) are underway to study the influence of cladding hydrogen distribution and hold time at high power on the mechanisms for outside-in cladding failure.

## ACKNOWLEDGEMENT

Financial support from the Swedish Foundation for Strategic Research (SSF) is gratefully acknowledged.

## REFERENCES

Alvarez-Holston, A. M., Grigoriev, V., Lysell, G., Källström, R., Johansson, B., Hallstadius, L., Zhou, G., Arimescu, I. and Lloret, M. (2010). "A combined approach to predict the sensitivity of fuel cladding to hydrogen-induced failures during power ramps," *Proc., 2010 LWR Fuel Performance Meeting*, American Nuclear Society, La Grange Park, IL, USA.

Cox, B. (1990). "Pellet-clad interaction (PCI) failures of zirconium alloy fuel cladding – a review," *J. Nucl. Mat.*, 172, 249-292.

Eadie, R.L., Tashiro, K., Harrington, D. and Léger, M. (1992). "The determination of the partial molar volume of hydrogen in zirconium in a simple stress gradient using comparative microcalorimetry," *Scr. Metallurgica et Materialia*, 26, 231-236.

Efsing, P. and Pettersson, K. (2000). "Delayed hydride cracking in irradiated Zircaloy cladding," *Zirconium in the nuclear industry: Twelfth international symposium, ASTM STP-1354*, G.P. Sabol and G.D. Moan (eds), American Society for Testing and Materials, 340-355.

Hagrman, D.L., Reymann, G.A. and Mason, R.E. (1981). "MATPRO-version 11 (revision 2) – a handbook of materials properties for use in the analysis of light water reactor fuel rod behavior," *Report NUREG/CR-0479*, United States Nuclear Regulatory Commission.

Hayashi, H., Etoh, Y., Tsukuda, Y., Shimada, S. and Sakurai, H. (2003). "Outside-in failure of BWR segment rods during power ramp tests," *Report IAEA TECDOC 1345, Part 1,* International Atomic Energy Agency, Vienna, Austria, 148-163.

Hayashi, H., Ogata, K., Baba, T. and Kamimura, K. (2006). "Research program to elucidate outside-in failure of high burnup fuel cladding," *J. Nucl. Sci. Techn.*, 43(9), 1128-1135.

Jernkvist, L.O. and Massih, A.R. (2007). "A numerical model for delayed hydride cracking of zirconium alloy cladding tubes," *Proc., SMiRT 19*, Aug. 12-17, 2007, Toronto, ON, Canada, Paper C01/3.

Kammenzind, B. F., Franklin, D. G., Peters, H. R. and Duffin, W. J. (1996). "Hydrogen pickup and redistribution in alpha-annealed Zircaloy-4," *Zirconium in the nuclear industry: Eleventh international symposium, ASTM STP-1295*, E.R. Bradley and G.P. Sabol (eds), American Society for Testing and Materials, 338-370.

Kanninen, M.F. and Popelar, C.H. (1985). *Advanced fracture mechanics*, Oxford University Press.

Li, J.C.M., Oriani, R.A. and Darken, L.S. (1966). "The thermodynamics of stressed solids," *Zeitschrift für Physikalische Chemie, Neue Folge*, 49, 271-291.

NEI (2004). "Fuel review," *Nuclear Engineering International*, September 2004 Issue, 26-35.

Ogata, K., Baba, T., Kamimura, K., Higuchi, T., Sakamoto, K., Etoh, Y. and Ito, K. (2009). "Effects of heat flux on hydrogen diffusion and hydride induced crack propagation in Zr-lined Zircaloy-2 cladding tube," *Proc., TopFuel 2009*, European Nuclear Society, Brussels, Belgium.

Puls, M.P. (2012). *The effect of hydrogen and hydrides on the integrity of zirconium alloy components: delayed hydride cracking*, Springer, London, UK.

Rice, J.R. and Rosengren, G.F. (1968). "Plane strain deformation near a crack tip in a power-law hardening material," *J. Mech. Phys. Solids*, 16, 1-12.

Sawatzky, A. (1960). "Hydrogen in Zircaloy-2: Its distribution and heat of transport," *J. Nucl. Mat*, 2, 321-328.

Shewmon, P. (1989). *Diffusion in solids, 2nd ed.*, The Minerals, Metals and Materials Society, TMS, Warrendale, PA, USA.

Shimada, S., Etoh, E., Hayashi, H. and Tukuta, Y. (2004). "A metallographic and fractographic study of outside-in cracking caused by power ramp tests," *J. Nucl. Mat.*, 327(2-3), 97-113.

Takagi, I., Hattori, T., Hashizumi, M. and Higashi, K. (1996). "Deuterium radial redistribution in Zr-liner cladding tubes," *Nucl. Instruments and Methods in Phys. Res. B*, B118, 238-241.

Une, K. and Ishimoto, S. (2004). "Terminal solid solubility of hydrogen in unalloyed zirconium by differential scanning calorimetry," *J. Nucl. Sci. Techn.*, 41, 949-952.

Une, K., Ishimoto, S., Etoh, Y., Ito, K., Ogata, K., Baba, T., Kamimura, K. and Kobayashi, Y. (2009). "The terminal solid solubility of hydrogen in irradiated Zircaloy-2 and microscopic modeling of hydride behavior," *J. Nucl. Mat.*, 389, 127-136.

Zinkle, S.J. and Was, G.S. (2013). "Materials challenges in nuclear energy," *Acta Materialia*, 61, 735-758.